

The evolution of the ion diffusion region during collisionless magnetic reconnection in a force-free current sheet

Fushun Zhou, Can Huang, Quanming Lu, Jinlin Xie, and Shui Wang

Citation: *Physics of Plasmas* **22**, 092110 (2015); doi: 10.1063/1.4930217

View online: <http://dx.doi.org/10.1063/1.4930217>

View Table of Contents: <http://scitation.aip.org/content/aip/journal/pop/22/9?ver=pdfcov>

Published by the *AIP Publishing*

Articles you may be interested in

[Effect of inflow density on ion diffusion region of magnetic reconnection: Particle-in-cell simulations](#)

Phys. Plasmas **18**, 111204 (2011); 10.1063/1.3641964

[Model of electron pressure anisotropy in the electron diffusion region of collisionless magnetic reconnection](#)

Phys. Plasmas **17**, 122102 (2010); 10.1063/1.3521576

[Structures of diffusion regions in collisionless magnetic reconnection](#)

Phys. Plasmas **17**, 052103 (2010); 10.1063/1.3403345

[Multispacecraft observations of the electron current sheet, neighboring magnetic islands, and electron acceleration during magnetotail reconnectiona\)](#)

Phys. Plasmas **16**, 056501 (2009); 10.1063/1.3112744

[The bimodal distribution structure of electron density brought about by the Hall effect in the electron diffusion region during magnetic reconnection](#)

Phys. Plasmas **14**, 062901 (2007); 10.1063/1.2741241



Trek
www.trekinc.com

HIGH-VOLTAGE AMPLIFIERS AND ELECTROSTATIC VOLTMETERS

ENABLING RESEARCH AND INNOVATION IN DIELECTRICS, MICROFLUIDICS, MATERIALS, PLASMAS AND PIEZOS

The evolution of the ion diffusion region during collisionless magnetic reconnection in a force-free current sheet

Fushun Zhou,^{1,2} Can Huang,^{1,2,a)} Quanming Lu,^{1,2} Jinlin Xie,³ and Shui Wang^{1,2}

¹CAS Key Laboratory of Geospace Environment, Department of Geophysics and Planetary Science, University of Science and Technology of China, Hefei 230026, China

²Collaborative Innovation Center of Astronautical Science and Technology, Harbin 150001, China

³CAS Key Laboratory of Geospace Environment, Department of Modern Physics, University of Science and Technology of China, Hefei 230026, China

(Received 10 May 2015; accepted 20 August 2015; published online 14 September 2015)

Two-dimensional particle-in-cell simulation is performed to investigate magnetic reconnection in a force-free current sheet. The results show that the evolution of the ion diffusion region has two different phases. In the first phase, the electrons flow toward the X line along one pair of separatrices and away from the X line along the other pair of separatrices. Therefore, in the ion diffusion region, a distorted quadrupole structure of the out-of-plane magnetic field is formed, which is similar to that of a typical guide field reconnection in the Harris current sheet. In the second phase, the electrons move toward the X line along the separatrices and then flow away from the X line at the inner side of the separatrices. In the ion diffusion region, the out-of-plane magnetic field exhibits a characteristic quadrupole pattern with a good symmetry, which is similar to that of antiparallel reconnection in the Harris current sheet. © 2015 AIP Publishing LLC.

[<http://dx.doi.org/10.1063/1.4930217>]

I. INTRODUCTION

Magnetic reconnection is a fundamental physical process that rapidly converts magnetic energy into plasma kinetic and thermal energies.^{1–3} At the same time, the process involves topological changes of the magnetic field lines.^{4–6} Magnetic reconnection has been used to explain many bursts phenomena in the solar atmosphere,^{7,8} the Earth's magnetosphere,^{9–11} and laboratory plasma.¹² It is generally accepted that the conversion from magnetic energy to plasma kinetic and thermal energies during magnetic reconnection happens in the diffusion region. The diffusion region in collisionless magnetic reconnection has recently been found to have multi-scale structures, which is determined by the Hall effect.^{6,13–16} At the scale length below the ion inertial length, which is called as ion diffusion region, the ions are decoupled from magnetic field lines, while the electrons are still frozen in the field lines. At the scale length below the electron inertial length, which is called as electron diffusion region, both the ions and electrons become demagnetized.

The structure of the ion diffusion region in collisionless magnetic reconnection is sensitive to the initial guide field.^{6,17,18} In antiparallel reconnection, the electrons move toward the X line along the separatrices due to the effects of the magnetic mirror, and then flow away from the X line along the magnetic field lines at the inner side of the separatrices. The electron density depletion layers are formed along the separatrices.^{6,16} These features have been confirmed by spacecraft observations.^{19–22} Therefore, the in-plane Hall

currents are directed away from the X line along the separatrices, and toward the X line just at the inner side of the separatrices.^{6,23,24} The quadrupole structure of the out-of-plane Hall magnetic field is considered to be caused by such a current system.^{6,13,16–18,24–26} With the increase of the initial guide field, the symmetry of the out-of-plane magnetic field and electron density depletion layers is distorted.^{18,24,27,28} When the initial guide field is sufficiently strong, the electrons are accelerated towards the X line along one pair of separatrices by the parallel electric field and then they are directed away from the X line along the other pair.¹⁸ Consequently, the electron density depletion layers are formed along the separatrices with the inflow electrons, and the resulted current system enhances the out-of-plane magnetic field in the center of the current sheet of the outflow region.¹⁸ These conclusions are obtained from simulations of collisionless magnetic reconnection in the Harris current sheet. Nevertheless, in interplanetary or solar wind, where the plasma β is much smaller than one, a force-free current sheet should be considered. Previous studies associated with a force-free current sheet focused on the excitation of plasma instabilities and the dissipation process of the magnetic field energy in the current sheet.^{29–32} In this paper, with two-dimensional (2D) particle-in-cell (PIC) simulations, we study the evolution of the ion diffusion region during collisionless magnetic reconnection in a force-free current sheet, and find that the ion diffusion region has two distinct phases during its evolution, which is quite different from that in the Harris current.

The paper is organized as follows: in Sec. II, we present the 2D PIC simulation model. In Sec. III, we show simulation results. The conclusions and discussion are given in Sec. IV.

^{a)}Author to whom correspondence should be addressed. Electronic mail: canhuang@mail.ustc.edu.cn

II. SIMULATION MODEL

A 2D PIC simulation code is used in this paper to investigate the evolution of the ion diffusion region during collisionless magnetic reconnection in a force-free current sheet. In the simulation, the electromagnetic fields are defined on the grids and updated by solving the Maxwell equations with a full explicit algorithm. In our simulation model, the initial condition is a force-free current layer with $\mathbf{B} = B_0 \tanh[(z - \frac{L_z}{2})/\delta] \mathbf{e}_x + B_0 \operatorname{sech}[(z - \frac{L_z}{2})/\delta] \mathbf{e}_y$, where B_0 is the asymptotical magnetic strength. δ is the half-width of the current sheet. L_z is the size of the simulation domain in the z direction. The current sheet width is $\delta = 0.5\lambda_i = 0.5c/\omega_{pi}$, where λ_i is the ion inertial length defined by n_0 . The mass ratio is set to be $m_i/m_e = 100$. The light speed is $c = 20v_A$, where v_A is the Alfvén speed defined by B_0 and n_0 . Note that here we use the initial particle distributions proposed by Bobrova *et al.*,²⁹ who demonstrate that the force-free configuration of a current sheet can exist when at least one plasma species has a temperature anisotropy. This is quite different from the usually considered Harris current sheet. The initial electron temperature ratio in this study is chosen as $T_{e\parallel}/T_{e\perp} = 1.1$, while the electron drift velocity is set to be $2v_A$, and the Buneman instability cannot be excited in this situation.

The computation is carried out in a rectangular domain in the (x, z) plane with dimension $L_x \times L_z = 102.4\lambda_i \times 25.6\lambda_i$. An $N_x \times N_z = 2048 \times 512$ grid system is employed in the simulation, so the spatial resolution is $\Delta x = \Delta z = 0.05c/\omega_{pi} = 0.5c/\omega_{pe}$. The time step is $\Omega_i \Delta t = 0.001$, where Ω_i is the ion gyrofrequency. We employ more than 10^8 particles per species. The periodic boundary conditions are used along the x direction, while the ideal conducting boundary conditions for electromagnetic fields and reflected boundary conditions for particles are employed in the z direction. In order to make the system enter the nonlinear stage quickly, an initial flux perturbation is introduced, which is useful to reach the stage with a rapid growth. Although the force-free state is the local minimum energy state according to the Taylor's theorem, an initial perturbation applied in the simulation may make it accessible an adjacent state with a lower energy, and then the magnetic energy is released.³²

III. SIMULATION RESULTS

In this paper, we perform a 2D PIC simulation to investigate the evolution of the ion diffusion region during collisionless magnetic reconnection in a force-free current sheet. Figure 1 shows the time evolution of the reconnection magnetic flux $\Delta\psi$ and the calculated reconnection electric field E_R at the X line. Here, $\Delta\psi$ is defined as the flux difference between the X and O lines, and its slope indicates the rate of magnetic reconnection. Both the magnetic flux $\Delta\psi$ and reconnection electric field E_R begin to increase around $\Omega_i t = 15$, and it means that the magnetic field begins to reconnection at that time. Around $\Omega_i t = 30$, the reconnection electric field E_R reaches its maximum, which is about $0.08 V_A B_0$. The maximum value of the reconnection electric field is similar to that of antiparallel magnetic reconnection

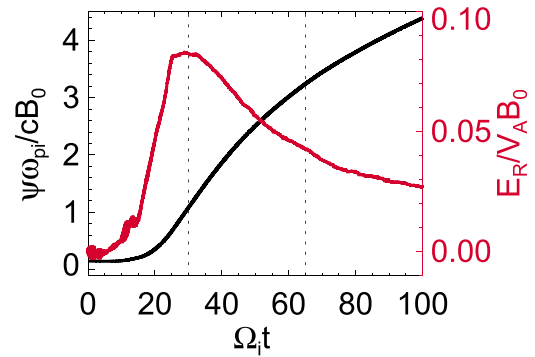


FIG. 1. The time evolution of the reconnection magnetic flux and the electric field. The dotted lines denote the time at $\Omega_i t = 30$ and 65 .

in the Harris current sheet. However, the reconnection rate normalized by the initial parameter is changing during the evolution of reconnection, and it reduces after attaining the maximum value. This can be found in the simulations of other works.^{17,26} One possible explanation is that with the evolution of the reconnection, the magnitude of the magnetic field in the upstream decreases due to the flux loss. Considering the evolution of the magnetic field in the upstream, we can find that the reconnection rate normalized with the parameters at that time, it is almost a constant.

Figure 2 shows the time evolution of the out-of-plane magnetic field B_y and the electric field in the z direction E_z . The magnetic field lines are also plotted in the figure for reference. Initially, the out-of-plane magnetic field B_y has a positive value in the current sheet. As the magnetic field begins to reconnection, B_y is pushed away from the vicinity of the X line, which is around $x = 0$. At the same time, the regions with a negative value of B_y begin to be formed along a pair of separatrices from the upper-left to the lower-right corner. This can be seen clearly in Fig. 2(c), and B_y with a positive value still occupies most of the region in the diffusion region. Such a structure of the out-of-plane magnetic field B_y is similar to that of guide field reconnection in the Harris current sheet, which is a distorted quadrupole pattern. The structure of E_z is also similar to that of guide field reconnection in the Harris current sheet: In the left of the X line, E_z is negative in the upper part and positive in the lower part of the current sheet, and the region with a positive E_z is larger than that with a negative E_z ; in the right of the X line, E_z is also negative in the upper part and positive in the lower part of the current sheet—however, the region with a negative E_z is larger than that with a positive E_z . With the proceeding of magnetic reconnection, the positive B_y is pushed more away from the vicinity of the X line, and B_y with a positive value begins to be formed in the regions along the other pair of separatrices from the lower-left to the upper-right corner. Therefore, a quadrupole structure of the out-of-plane magnetic field B_y with a good symmetry is formed in the ion diffusion region, as plotted in Fig. 2(d). At the same time, E_z also becomes symmetric along the center of the current sheet in both the left and right parts of the X line. Such structures of both B_y and E_z are similar to those of antiparallel reconnection in the Harris current sheet.⁶

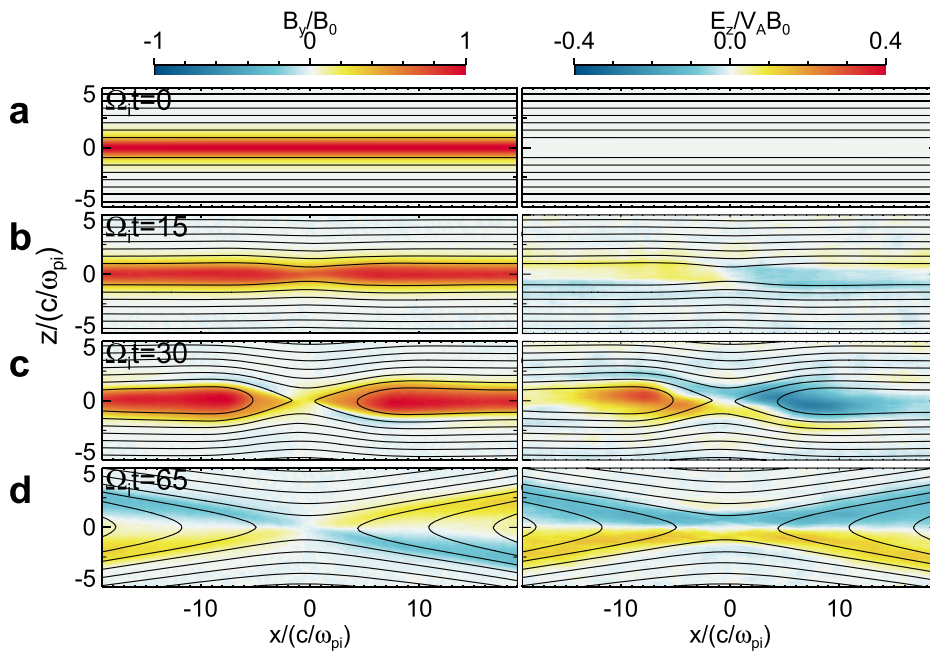


FIG. 2. The time evolution of the out-of-plane magnetic field B_y and the electric field in the z direction E_z , at (a) $\Omega_i t = 0$, (b) $\Omega_i t = 15$, (c) $\Omega_i t = 30$, and (d) $\Omega_i t = 65$. The magnetic field lines are also plotted in the figure.

To identify the generation mechanism of the out-of-plane magnetic field, we analyze the ion and electron flows in the ion diffusion region. Figure 3 plots the contours of (a) the out-of-plane magnetic field B_y , (b) the electron density n_e , (c) the ion flow vectors, and (d) the electron flow vectors at $\Omega_i t = 30$. The ion flow toward the X line is driven by the reconnection electric field in the form of the $\mathbf{E} \times \mathbf{B}$ drift, and then they are directed away from the X line almost along the x direction. The electrons, on the other hand, flow toward the X line along the pair of the separatrices from the lower left to the upper right corner, and then are away from the X line along the magnetic field lines just inside the pair of the separatrices from the upper left to the lower right corner. Such a pattern of the electron flow leads to an obvious depletion of the electron density along the pair of the separatrices from the lower left to the upper right corner. These structures can be demonstrated more clearly in Figure 4, which depicts the profiles of the out-of-plane magnetic field B_y , the electron

density n_e , the electron bulk velocity, and the curl of the non-ideal electric field in the ion frame along $x = -3c/\omega_{pi}$ at $\Omega_i t = 30$. The out-of-plane magnetic field is asymmetric in the z direction, and the electron outflow is stronger than the inflow. The minimum of the electron density appears around $z = -1.5c/\omega_{pi}$, which is also the peak of the electron flow velocities. Here, the existence of the out-of-plane magnetic field in the current sheet, which plays the similar role of the guide field in guide field reconnection in the Harris current sheet, leads to the resulted structures of the flow pattern and electron density, and then the structures of the out-of-plane magnetic field and electric field. Please note that the ion bulk velocity is much smaller than the electron bulk velocity, and the in-plane current is determined mostly by the electron flow.⁶ The formation of such a structure of the out-of-plane magnetic field due to such an electron flow is similar to that in the Harris current sheet with a guide field, and the details can be found in Refs. 18 and 33. The curl of

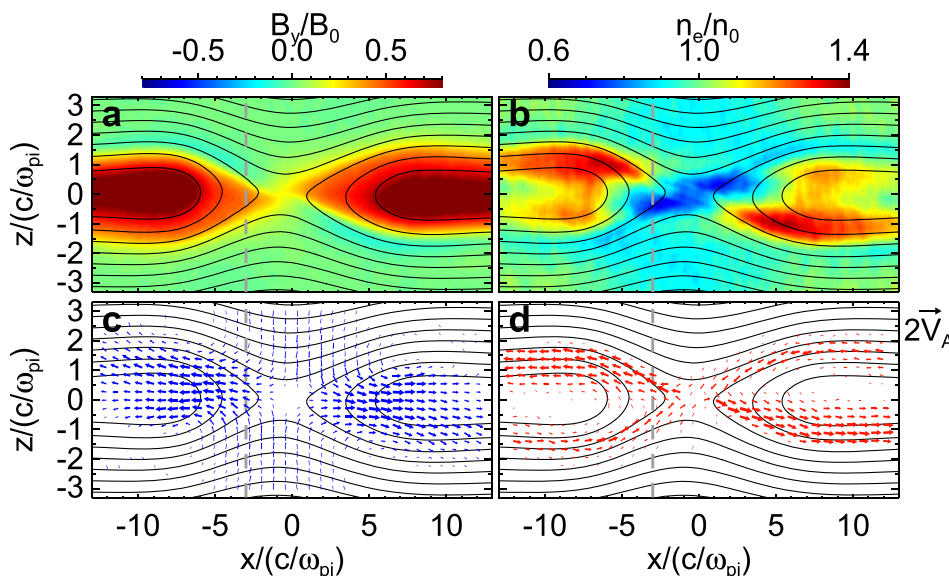


FIG. 3. The contours of (a) the out-of-plane magnetic field B_y , (b) the electron density n_e , (c) the ion flow vectors, and (d) the electron flow vectors at $\Omega_i t = 30$. The in-plane magnetic field lines are also plotted in the figure.

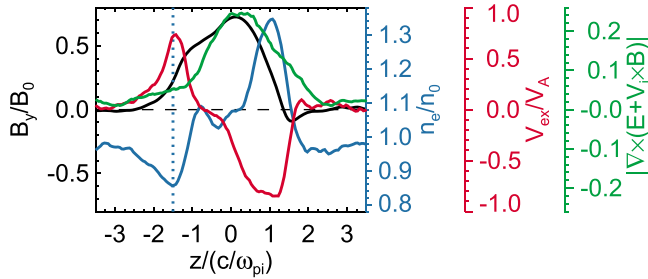


FIG. 4. The profiles of the out-of-plane magnetic field B_y (black), the electron density n_e (blue), the electron flow velocities in the x direction (red), and the curl of the non-ideal electric field in the ion frame (green) along $x = -3c/\omega_{pi}$ at $\Omega_i t = 30$. The dotted line denotes the position with the minimal electron density.

the non-ideal electric field is usually considered to be the criterion of the diffusion region. When $\nabla \times (\mathbf{E} + \mathbf{V}_i \times \mathbf{B})$ is non-zero, ions are decoupled with the field lines. It is clear that the perturbed out-of-plane magnetic fields are covered by the region where $\nabla \times (\mathbf{E} + \mathbf{V}_i \times \mathbf{B})$ is sufficiently large.

Figure 5 plots the contours of (a) the out-of-plane magnetic field B_y , (b) the electron density n_e , (c) the ion flow vectors, and (d) the electron flow vectors at $\Omega_i t = 65$. At this time, the out-of-plane magnetic field B_y , which exists initially in the current sheet, is pushed farther away from the vicinity of the X line. The out-of-plane magnetic field B_y exhibits a quadrupole pattern with a good symmetry in the ion diffusion region around the X line. The electrons flow toward the X line along the separatrices, and then they flow away from the X line along the magnetic lines just inside the separatrices, while the ion flow is similar to that at $\Omega_i t = 30$. The electron density depletion layers are formed along the separatrices. These structures can be demonstrated more clearly in Figure 6, which depicts the profiles of the out-of-plane magnetic field B_y , the electron density n_e , the electron bulk velocity, and the curl of the non-ideal electric field in the ion frame along $x = -10c/\omega_{pi}$ at $\Omega_i t = 65$. The electron bulk velocities are much larger than the ion bulk velocities in the ion diffusion region and determine the in-plane current.⁶ Here, because the initial out-of-plane

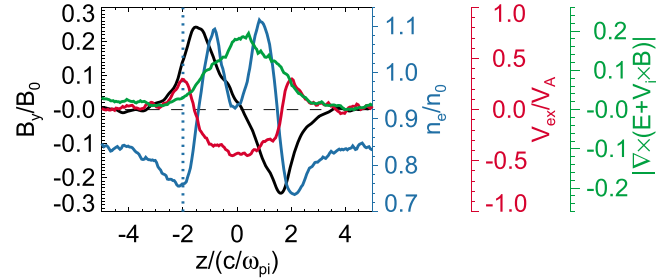


FIG. 6. The profiles of the out-of-plane magnetic field B_y (black), the electron density n_e (blue), the electron flow velocities in the x direction (red), and curl of the non-ideal electric field in the ion frame (green) along $x = -10c/\omega_{pi}$ at $\Omega_i t = 65$. The dotted line denotes the position with the minimal electron density.

magnetic field has been pushed away from the ion diffusion region, the structures of the electric and magnetic field are similar to those of anti-parallel magnetic reconnection in the Harris current sheet, which have a good symmetry.

IV. CONCLUSIONS AND DISCUSSION

In this paper, with a 2D PIC simulation, we investigate the evolution of the ion diffusion region of magnetic reconnection in a force-free current sheet. The process of magnetic reconnection has two different phases. In the first phase, the electrons flow toward the X line along one pair of the separatrices from the lower left to the upper right corner, and the high speed electrons flow away from the X line along the magnetic field lines inside the other pair of separatrices from the upper left to the lower right corner, where a depletion layer is formed. The resulted in-plane Hall current leads to a distorted quadrupole structure of the out-of-plane magnetic field: a negative value of the out-of-plane magnetic field exists in the pair of separatrices from the upper left to the lower right corner, while a positive value of the out-of-plane magnetic field occupies most part of the ion diffusion region. Such a structure of the out-of-plane magnetic field is similar to that of guide field reconnection in the Harris current sheet. In the second phase, the electrons move toward the X line

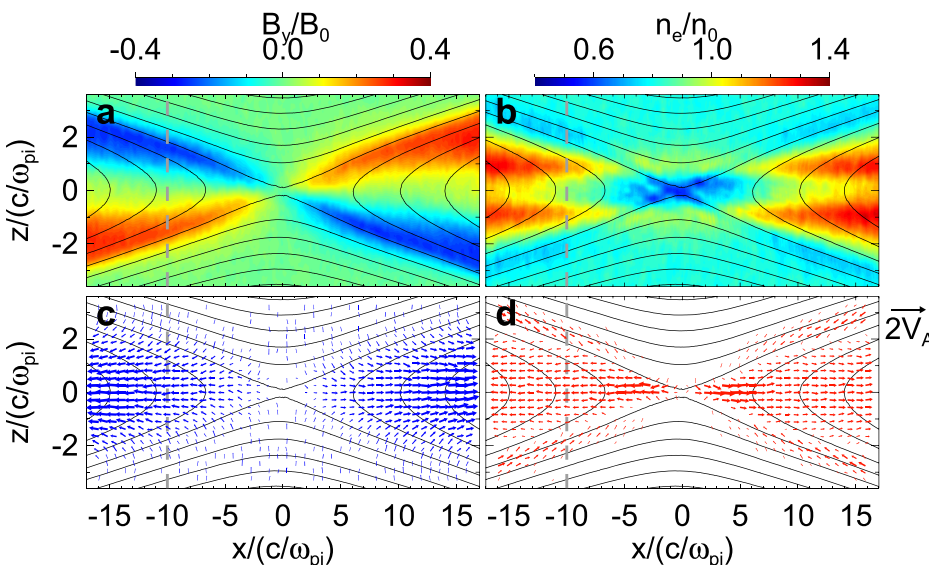


FIG. 5. The contours of (a) the out-of-plane magnetic field B_y , (b) the electron density n_e , (c) the ion flow vectors, and (d) the electron flow vectors at $\Omega_i t = 65$. The in-plane magnetic field lines are also plotted in the figure.

along the separatrices, and then they are directed away from the X line along the magnetic field lines just inside the separatrices, which leads to symmetric electron density depletion layers along the separatrices. The resulted current system causes the characteristic quadrupole pattern of the out-of-plane magnetic field in the ion diffusion region, which exhibits a good symmetry.

Recently, reconnection events have been *in situ* observed in the interplanetary space,³⁴ where the current sheets may have a force-free configuration, and the electron acceleration during reconnection in a force-free current sheet is getting more and more attention.^{35,36} Previous simulations of magnetic reconnection in the Harris current sheet with a guide field have shown that electrons are accelerated by a parallel electric field in the vicinity of the X line, and the acceleration efficiency is enhanced because these electrons can stay longer time in the vicinity of the X line due to the gyration in the guide field.^{17,24} In this paper, we find that the structure of the out-of-plane magnetic field is changing during magnetic reconnection in a force-free current sheet. In the first phase, a distorted quadrupole structure of the out-of-plane magnetic field is formed, which is similar to that of a typical guide field reconnection in the Harris current sheet. In the second phase, the out-of-plane magnetic field exhibits a characteristic quadrupole pattern with a good symmetry, which is similar to that of antiparallel reconnection in the Harris current sheet. Therefore, the process of electron acceleration during magnetic reconnection in a force-free current sheet may be different from that in the Harris current sheet, which is our future investigation.

ACKNOWLEDGMENTS

This research was supported by the National Science Foundation of China, Grant Nos. 41331067, 41204103, 11220101002, 11235009, 41274144, 41121003, 973 Program (2013CBA01503, 2012CB825602), Ph.D. Programs Foundation of Ministry of Education of China (20123402120010), and CAS Key Research Program KZZD-EW-01-4.

¹P. A. Sweet, in *Electromagnetic Phenomena in Cosmical Physics*, edited by B. Lehnert (Cambridge University Press, New York, 1957), p. 123.

²E. N. Parker, *J. Geophys. Res.* **62**, 509, doi:10.1029/JZ062i004p00509 (1957).

³V. M. Vasyliunas, *Rev. Geophys. Space Phys.* **13**, 303, doi:10.1029/RG013i001p00303 (1975).

⁴E. Priest and T. Forbes, *Magnetic Reconnection: MHD Theory and Applications* (Cambridge University Press, Cambridge, 2000).

⁵R. S. Wang, Q. M. Lu, A. M. Du, and S. Wang, *Phys. Rev. Lett.* **104**, 175003 (2010).

⁶Q. M. Lu, C. Huang, J. L. Xie, R. S. Wang, M. Y. Wu, A. Vaivads, and S. Wang, *J. Geophys. Res.* **115**, A11208, doi:10.1029/2010JA015713 (2010).

⁷R. G. Giovanelli, *Nature (London)* **158**, 81 (1946).

⁸P. Ulmschneider, E. R. Priest, and R. Rosner, in *Mechanisms of Chromospheric and Coronal Heating*, edited by R. Rosner (Springer-Verlag, Berlin, 1991).

⁹A. Nishida, *Geomagnetic Diagnostics of the Magnetosphere* (Springer-Verlag, New York, 1978).

¹⁰W. J. Hughes, in *Introduction to Space Physics*, edited by M. G. Kivelson and C. T. Russell (Cambridge University Press, New York, 1995), p. 227.

¹¹Z. Y. Pu, X. N. Chu, X. Cao, V. Mishin, V. Angelopoulos, J. Wang, Y. Wei, Q. G. Zong, S. Y. Fu, L. Xie, K.-H. Glassmeier, H. Frey, C. T. Russell, J. Liu, J. McFadden, D. Larson, S. Mende, I. Mann, D. Sibeck, L. A. Sapronova, M. V. Tolochko, T. I. Saifudinova, Z. H. Yao, X. G. Wang, C. J. Xiao, X. Z. Zhou, H. Reme, and E. Lucek, *J. Geophys. Res.* **115**, A02212, doi:10.1029/2009JA014217 (2010).

¹²J. Wesson, *Tokomaks* (Oxford Univ. Press, New York, 1997).

¹³B. U. Ö. Sonnerup, "Magnetic field reconnection," in *Solar System Plasma Physics*, edited by L. J. Lanzerotti, C. F. Kennel, and E. N. Parker (North-Holland, New York, 1979), Vol. 3, p. 46.

¹⁴J. Birn, J. F. Drake, M. A. Shay, B. N. Rogers, R. E. Denton, M. Hesse, M. Kuznetsova, Z. W. Ma, A. Bhattacharjee, A. Otto, and P. L. Pritchett, *J. Geophys. Res.* **106**, 3715, doi:10.1029/1999JA900449 (2001).

¹⁵M. A. Shay, J. F. Drake, B. N. Rogers, and R. E. Denton, *J. Geophys. Res.* **106**, 3759, doi:10.1029/1999JA001007 (2001).

¹⁶R. S. Wang, Q. M. Lu, C. Huang, and S. Wang, *J. Geophys. Res.* **115**, A01209, doi:10.1029/2009JA014553 (2010).

¹⁷X. R. Fu, Q. M. Lu, and S. Wang, *Phys. Plasmas* **13**, 012309 (2006).

¹⁸S. Lu, Q. M. Lu, Y. Cao, C. Huang, J. L. Xie, and S. Wang, *Chin. Sci. Bull.* **56**, 48 (2011).

¹⁹M. Øieroset, T. D. Phan, M. Fujimoto, R. P. Lin, and R. P. Lepping, *Nature* **412**, 414 (2001).

²⁰F. S. Mozer, S. D. Bale, and T. D. Phan, *Phys. Rev. Lett.* **89**, 015002 (2002).

²¹A. Vaivads, Y. Khotyaintsev, M. André, A. Retinò, S. C. Buchert, B. N. Rogers, P. Décreau, G. Paschmann, and T. D. Phan, *Phys. Rev. Lett.* **93**, 105001 (2004).

²²C. Cattell, J. Dombek, J. Wygant, J. F. Drake, M. Swisdak, M. L. Goldstein, W. Keith, A. Fazakerley, M. André, E. Lucek, and A. Balogh, *J. Geophys. Res.* **110**, A01211, doi:10.1029/2004JA010519 (2005).

²³T. Nagai, I. Shinohara, M. Fujimoto, S. Machida, R. Nakamura, Y. Saito, and T. Mukai, *J. Geophys. Res.* **108**, 1357, doi:10.1029/2003JA009900 (2003).

²⁴C. Huang, Q. M. Lu, and S. Wang, *Phys. Plasmas* **17**, 072306 (2010).

²⁵T. Nagai, I. Shinohara, M. Fujimoto, M. Hoshino, Y. Saito, S. Machida, and T. Mukai, *J. Geophys. Res.* **106**, 25929, doi:10.1029/2001JA900038 (2001).

²⁶P. L. Pritchett, *J. Geophys. Res.* **106**, 3783, doi:10.1029/1999JA001006 (2001).

²⁷B. N. Rogers, R. E. Denton, and J. F. Drake, *J. Geophys. Res.* **108**, 1111, doi:10.1029/2002JA009699 (2003).

²⁸P. L. Pritchett and F. V. Coroniti, *J. Geophys. Res.* **109**, A01220, doi:10.1029/2003JA009999 (2004).

²⁹N. A. Bobrova, S. V. Bulanov, J. I. Sakai, and D. Sugiyama, *Phys. Plasmas* **8**, 759 (2001).

³⁰J. I. Sakai, D. Sugiyama, T. Haruki, N. Bobrova, and S. Bulanov, *Phys. Rev. E* **63**, 046408 (2001).

³¹K. Nishimura, S. P. Gary, H. Li, and S. A. Colgate, *Phys. Plasmas* **10**, 347 (2003).

³²H. Li, K. Nishimura, D. C. Barnes, S. P. Gary, and S. A. Colgate, *Phys. Plasmas* **10**, 2763 (2003).

³³J. P. Eastwood, M. A. Shay, T. D. Phan, and M. Øieroset, *Phys. Rev. Lett.* **104**, 205001 (2010).

³⁴Y. Wang, F. S. Wei, X. S. Feng, S. H. Zhang, P. B. Zuo, and T. R. Sun, *Phys. Rev. Lett.* **105**, 195007 (2010).

³⁵F. Guo, H. Li, W. Daughton, and Y. H. Liu, *Phys. Rev. Lett.* **113**, 155005 (2014).

³⁶F. Guo, Y. H. Liu, W. Daughton, and H. Li, *Astrophys. J.* **806**, 167 (2015).